Quantum kinetics of electrons at plasma boundaries

Franz X. Bronold, Holger Fehske, Rafael L. Heinisch and Johannes Marbach

Institut für Physik, Ernst-Moritz-Arndt-Universität Greifswald, D-17489 Greifswald, Germany

TR ÷ 24 complex plasmas

1 Motivation [1, 2]

Macroscopic objects in contact with an ionized gas are negatively charged. They accumulate electrons more efficiently than ions leading to the build-up of a quasi-stationary electron film at the plasma boundary.
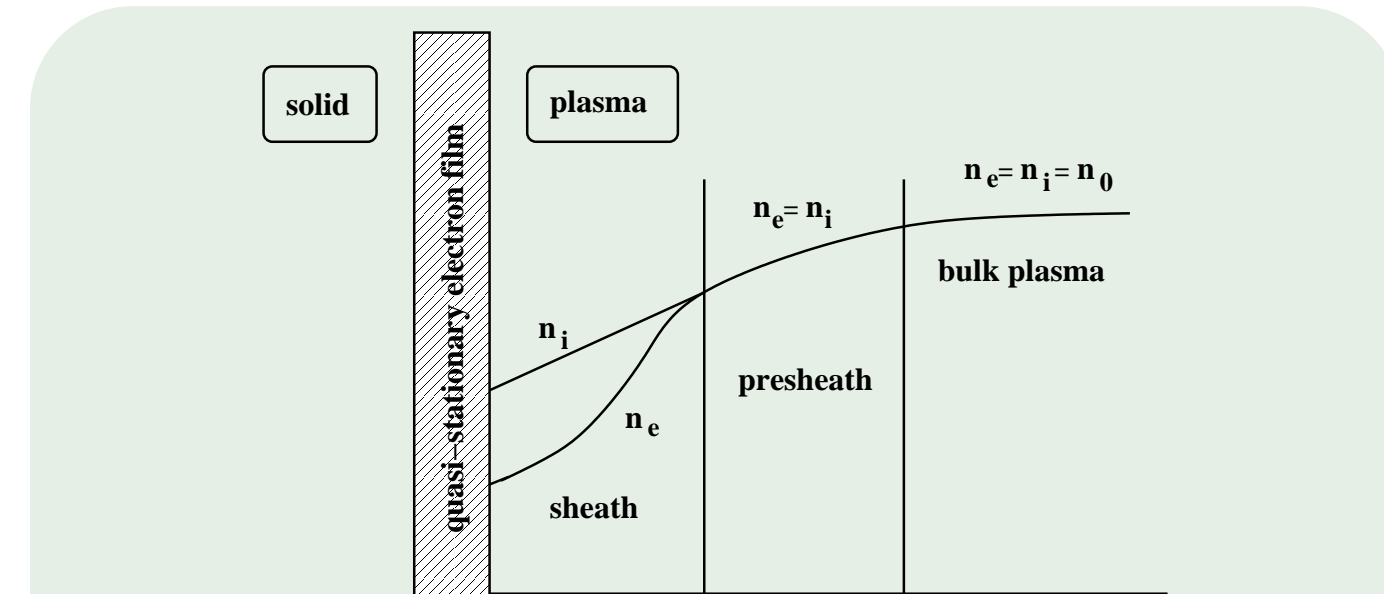

Fig. 1: *Spatial variation of the electron and ion density in a bounded plasma. In the bulk plasma, electron and ion density are equal and constant, in the presheath the two densities vary spatially but are still identical, in the sheath the electron density is strongly suppressed.*

The plasma is strongly affected by surface charges, via sheath formation (see Fig. 1), electron-ion recombination, and secondary electron emission. But, up to now, there is no microscopic theory answering questions of the following kind:

- What forces bind electrons to the plasma boundary and what controls electron energy dissipation at the boundary?
- What is the probability for an electron to stick at or to desorb from the plasma boundary?
- How do ions and neutrals interact with negatively charged plasma boundaries?

It is only until recently that we started a robust investigation of the electronic microphysics at plasma boundaries [1, 2, 3, 4]. Its main purpose is to obtain – from microscopic models – surface parameters, such as, the electron sticking coefficient s_e, the electron desorption time τ_e, and the secondary electron emission coefficient γ_e. All three are crucial for a complete kinetic description of bounded plasmas but little is known about them quantitatively.

2 Surface charges [2, 3]

Whenever at the plasma boundary the plasma potential falls inside an energy gap, a plasma electron approaching the boundary may get trapped (adsorbed) in external, polarization-induced surface states provided it can get rid of its excess energy. Once it is trapped it may de-trap again (desorb) if it gains enough energy from the surface.

Hence, in addition to elastic and inelastic scattering, the interaction of plasma electrons with boundaries encompasses physisorption – the polarization-induced temporary binding of an electron to the surface which may be characterized by s_e and τ_e. We propose that this process leads to the build-up of surface charges at plasma boundaries.

Below we focus on physisorption of electrons at metallic surfaces. Physisorption of electrons at dielectric surfaces has been studied in [3].

2.1 Microscopic model

Quite generally, a quantum-mechanical calculation of s_e and τ_e has to be based on a Hamiltonian,

$$H = H_e + H_b + H_{e-b}, \qquad (1)$$

where H_e and H_b describe the unperturbed dynamics of, respectively, the plasma electrons in the vicinity of the solid and the elementary excitations of the solid responsible for electron energy relaxation and H_{e-b} encodes the coupling between the two. For the calculation of s_e and τ_e it suffices to consider, in a first approximation, a planar, uncharged plasma boundary. It defines the xy-plane of a coordinate system separating the plasma in the halfspace $z > 0$ from the solid in the halfspace $z \leq 0$.

The microphysics of electrons specifically at a metallic boundary is schematically shown in Fig. 2. A plasma electron approaching the boundary in an extended state with $E > 0$ may be bound in a surface state with $E < 0$ provided it dissipates its excess energy to the internal electron-hole pairs of the metallic boundary. Similarly, an electron initially occupying a bound surface state may desorb from the surface when it gains enough energy to reach an extended state. The rate $\mathcal{W}$ for such transitions can be perturbatively obtained as shown in the inset.

We neglect polycrystallinity and chemical contamination of the plasma boundary and work with a per-

fect surface. Two types of surface states are then possible: Intrinsic surface states, originating from the abrupt appearance of the periodic lattice potential for $z < 0$ or unsaturated bonds at the surface and polarization-induced (image) states due to exchange and correlation effects for $z > 0$. Image states extend a few $Å$ into the plasma. We expect them to be most important for the build-up of surface charges and keep only these states. Approximating the polarization-induced potential by the classical image potential, the wavefunctions for the approaching plasma electron are Whittaker functions [2].
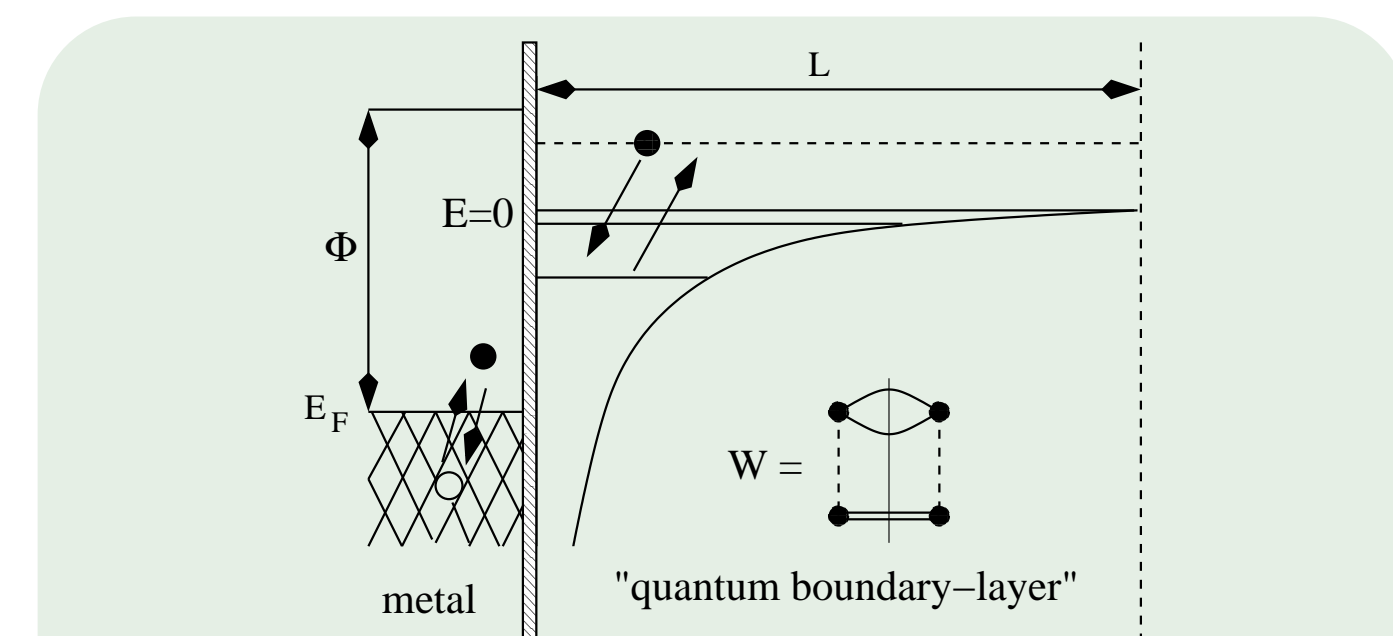

Fig. 2: *Microphysics of plasma electrons at metallic boundaries. L is the width of the "boundary layer" where quantum mechanics applies; Φ and E_F are, respectively, the work function and the Fermi energy of the metal.*

Plasma electrons loose/gain energy at metallic surfaces via creation/annihilation of internal electron-hole pairs. To describe this process we treat the boundary as a jellium halfspace interacting with plasma electrons via a screened Coulomb interaction: $V_s(r) \sim \exp[-(k_s)_{\text{surface}} r]/r$, where $(k_s)_{\text{surface}}$ is the screening wavenumber at the surface. Positron scattering experiments indicate $(k_s)_{\text{surface}} \approx 0.6 (k_s)_{\text{bulk}}$. Assuming an infinitely high barrier at $z = 0$, the wavefunctions for internal electrons are standing waves and H_{e-b} can be worked out analytically [2].

If τ_e is sufficiently long, plasma electrons bound in image states are in thermal equilibrium with the surface. The desorption rate is then given by

$$\frac{1}{\tau_e} = \frac{\sum_{\vec{Q}'n'}\sum_{\vec{Q}q}\exp[-\beta_s E_{\vec{Q}'n'}]\mathcal{W}(\vec{Q}q,\vec{Q}'n')}{\sum_{\vec{Q}n}\exp[-\beta_s E_{\vec{Q}n}]}, \quad (2)$$

where $T_s = (k_B \beta_s)^{-1}$ is the surface temperature and $\mathcal{W}(\vec{Q}q,\vec{Q}'n')$ is the transition rate from the bound surface state $(\vec{Q}',n')$, with $\vec{Q}'$ the lateral momentum and n' the vertical quantum number, to the extended surface state $(\vec{Q},q)$. The energy of the two states is, respectively, $E_{\vec{Q}'n'}$ and $E_{\vec{Q}q}$.

For an electron in an extended surface state the tendency to stick to any bound surface state is

$$S_{\vec{Q}'q'} = \frac{16 L m_e a_B}{\hbar q'} \sum_{\vec{Q}n} \mathcal{W}(\vec{Q}n,\vec{Q}'q'), \qquad (3)$$

where L is the width of the quantum-mechanical boundary layer (drops out for $L \to \infty$); m_e is the electron mass. Provided extended surface states are Maxwellian occupied, with a temperature $T_e = (k_B \beta_e)^{-1}$, the angle and energy averaged sticking coefficient – the global sticking coefficient s_e– is

$$s_e = \frac{\sum_{\vec{Q}'q'} S_{\vec{Q}'q'} q' \exp[-\beta_e E_{\vec{Q}'q'}]}{\sum_{\vec{Q}'q'} q' \exp[-\beta_e E_{\vec{Q}'q'}]}. \qquad (4)$$

2.2 Results

We modified the binding energies of the surface states as obtained from the classical image potential by an overall factor of 0.7. This factor was chosen to adjust the binding energy of the lowest surface state to the value measured for copper: $|E_1|^{\text{Cu}} \approx 0.6eV$. Assuming this modification to approximately account for the deviation of the true polarization-induced potential from the classical image potential, we used this value also for the other metals.
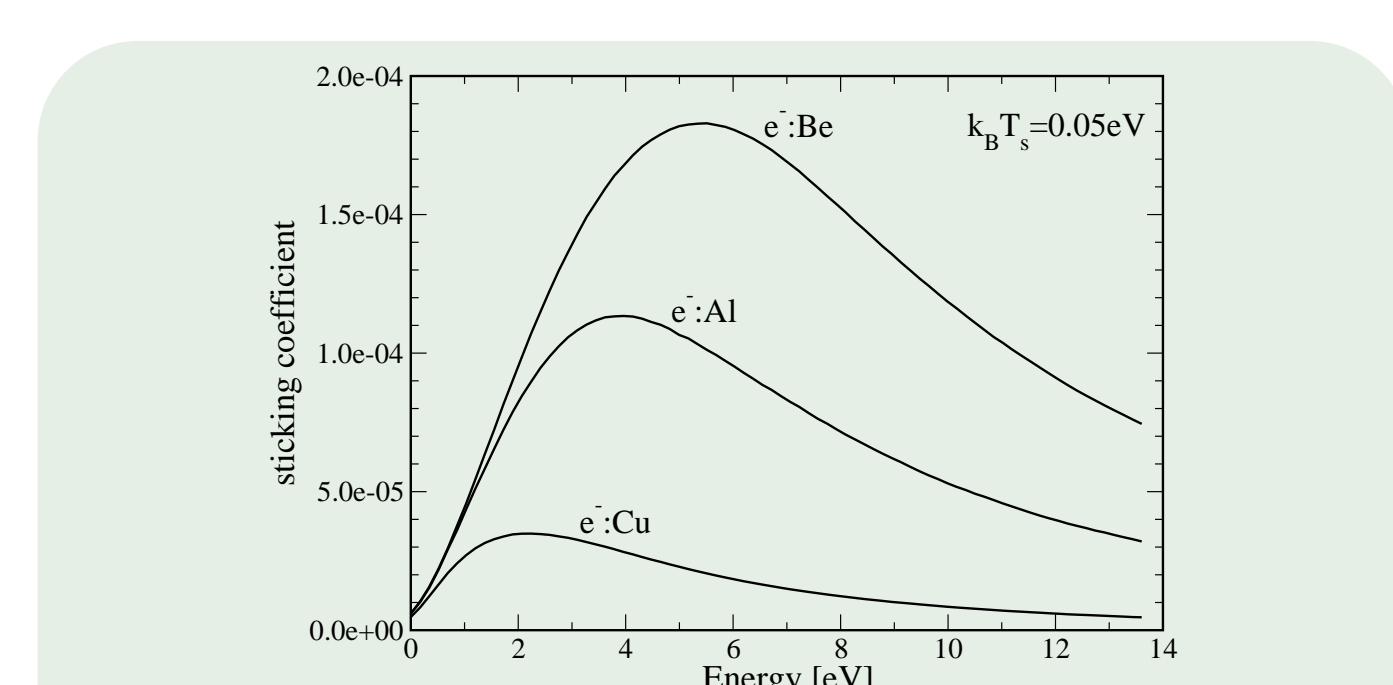

Fig. 3: *Energy resolved sticking coefficient for plasma electrons hitting perpendicularly, respectively, a copper, an aluminum, and a beryllium surface at $k_B T_s = 0.05 eV$.*

Figure 3 shows the energy resolved sticking coefficient when the plasma electron perpendicularly hits, respectively, a copper, an aluminum, and a beryllium

boundary at $kT_s = 0.05 eV$. The sticking coefficient turns out to be extremely small, of the order of 10^{-5}–10^{-4}. For weaker screening, and thus stronger coupling, we would obtain sticking coefficients as large as 10^{-1} but these screening wavenumbers are unphysical. Global sticking coefficients defined in (4) are also very small but the product $s_e \tau_e \approx 10^{-6}s$ (see Table 1), which is the order of magnitude we expect from our study of charging of dust particles in low-temperature gas discharges [1].

	Cu	Al	Be
$\tau_e[s]$	0.026	0.021	0.022
$s_e[10^{-5}]$	1.8	5.6	8.9
$s_e\tau_e[10^{-6}s]$	0.46	1.19	1.95

Table 1: *Electron desorption time and global sticking coefficient for a thermal beam of plasma electrons with $k_B T_e = 5eV$ hitting various metal surfaces at $k_B T_s = 0.05 eV$.*

3 Electron emission [4]

The secondary electron emission coefficient γ_e, that is, the total number of electrons released per particle impacting the plasma boundary, is an important surface parameter. It affects the electric breakdown of a gas and thus the operation mode of a gas discharge. Data about γ_e are however rather sparse, it has been hardly measured or calculated. Thus, in most plasma simulations γ_e is – by necessity – an adjustable parameter. Obviously this is an unacceptable situation.

For uncharged surfaces the processes leading to secondary electron emission are in principle known. In particular, de-excitation of metastable molecules at the surface is very efficient in producing secondary electrons either via Penning de-excitation (Auger de-excitation) or via resonant charge transfer and subsequent auto-ionization of the resulting temporary negative ion. At charged boundaries these processes should release both bulk and surface electrons.

In the following we focus on Penning de-excitation of metastable nitrogen molecules at an uncharged Al surface although this process is not directly related to gas discharges of current interest. It has been however previously studied and can thus be used to benchmark our approach. In N_2/O_2 dielectric barrier discharges the same process occurs at a Al_2O_3 surface (for which however no data are available).

3.1 Microscopic model

The microscopic model we adopt is schematically shown in Fig. 4. The metal electrons are treated as particles in a box with depth $V_0 = \Phi + E_F$, the released electron is assumed to be adequately given by a plane wave, and the metastable nitrogen molecule $N_2^*(^3\Sigma_u^+)$ is approximated by a (degenerate) two-level system using a $2\pi_u$ LCAO molecule orbital as the lower level and a $2\pi_g$ LCAO molecule orbital as the upper level with atomic orbitals obtained from a Coulomb potential with $Q = 7e$.
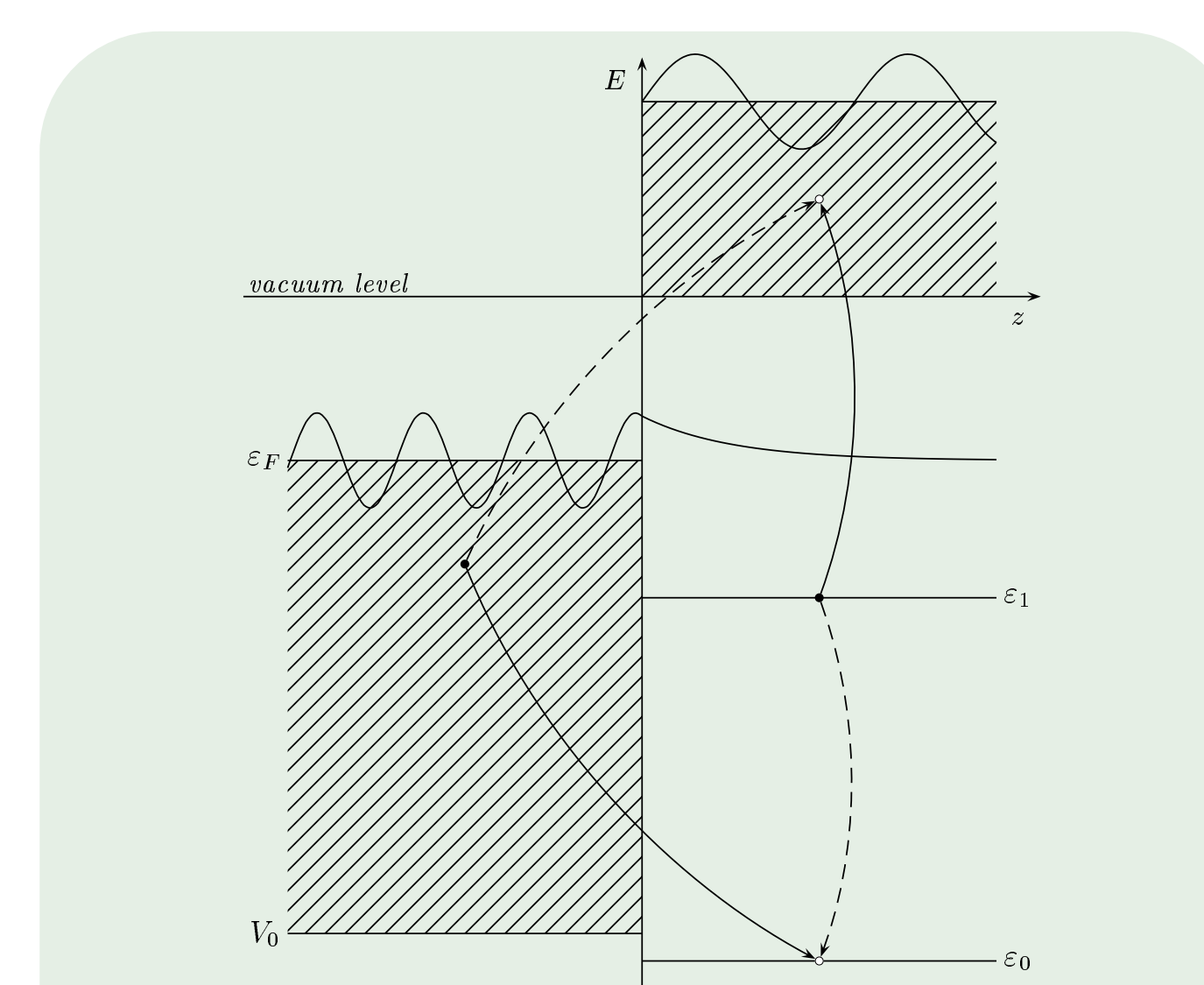

Fig. 4: *Penning de-excitation process (solid lines) in an Al/N_2^* system showing the electronic structure and the qualitative behavior of the electron wave functions. The Penning exchange process is indicated using dashed lines.*

In the trajectory approximation, the Hamiltonian describing Penning de-excitation (solid lines in Fig. 4) is given by (m denotes magnetic quantum number)

$$H = H_0 + H_1(t), \qquad (5)$$
$$H_0 = \sum_{\vec{k}} \epsilon_{\vec{k}} c_{\vec{k}}^\dagger c_{\vec{k}} + \sum_{\vec{q}} \epsilon_{\vec{q}} c_{\vec{q}}^\dagger c_{\vec{q}} + \sum_{i,m} \epsilon_i d_{im}^\dagger d_{im}, (6)$$
$$H_1(t) = \sum_{\vec{k},\vec{q},m} \left(V_{0m,\vec{k}}^{\vec{q},1m}(t) d_0^\dagger c_{\vec{k}} c_{\vec{q}}^\dagger d_1 + \text{h.c.} \right), \qquad (7)$$

where

$$V_{0m,\vec{k}}^{\vec{q},1m}(t) = \int d\vec{r} d\vec{s} \Psi_{0m}^*(\vec{r}) \Psi_{\vec{k}}(\vec{r} + \vec{R}(t)) V_c(\vec{r} - \vec{s})$$
$$\times \Psi_{\vec{q}}^*(\vec{s} + \vec{R}(t)) \Psi_{1m}(\vec{s}) \qquad (8)$$

is the time-dependent Coulomb interaction of the two active electrons involved in Penning de-excitation.

3.2 Quantum kinetics

To calculate γ_e we employ Keldysh Green functions. The decreasing lifetime of $N_2^*(^3\Sigma_u^+)$ when it approaches the boundary can then be easily included. In addition, the approach is flexible enough to deal with correlations on the molecule which is important when temporary negative ions are formed by resonant charge transfer.
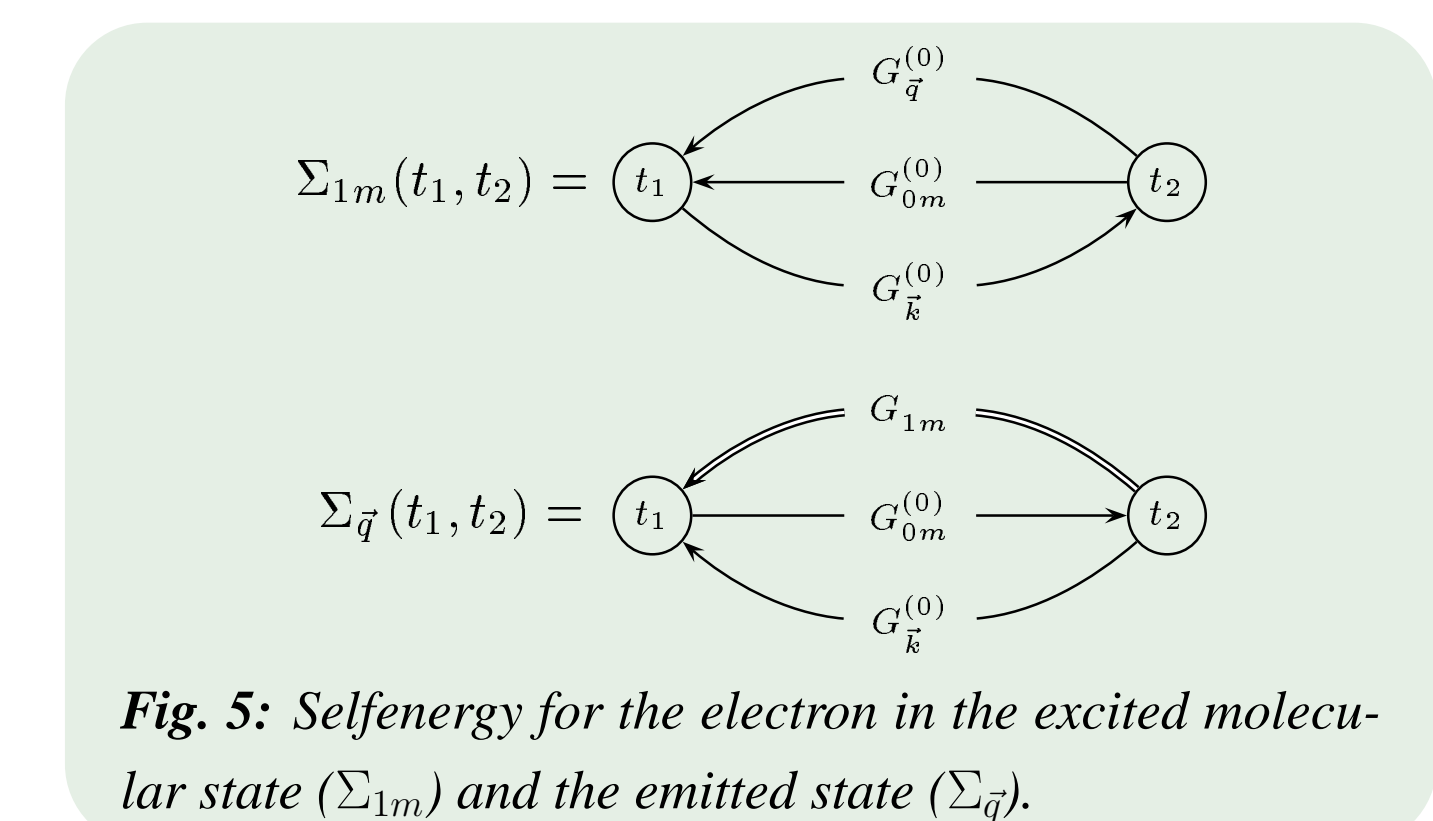

Fig. 5: *Selfenergy for the electron in the excited molecular state (Σ_{1m}) and the emitted state ($\Sigma_{\vec{q}}$).*

Initially there is no free electron with energy $\epsilon_{\vec{q}}$. Hence, γ_e is simply the overall occupancy of the free electron states after the collision is completed along the prescribed trajectory. In terms of Keldysh Green functions,

$$\gamma_e = \lim_{t\to\infty} \sum_{\vec{q}} n_{\vec{q}}(t)$$
$$= \lim_{t\to\infty} \frac{1}{2}\left[1 - i \sum_{\vec{q}} F_{\vec{q}}(t, t+0^+)\right], \qquad (9)$$

where, using the selfenergy diagrams shown in Fig. 5,

$$F_{\vec{q}}(t,t') = -\int d\bar{t}d\bar{\bar{t}} G_{\vec{q}}^{(0)R}(t,\bar{t})\Sigma_{\vec{q}}^{+-}(\bar{t},\bar{\bar{t}})G_{\vec{q}}^{(0)A}(\bar{\bar{t}},t') \qquad (10)$$

with $G^{(0)\cdots}_{\cdots}$ Green functions corresponding to H_0 and

$$\Sigma_{\vec{q}}^{+-}(t,t') = \sum_{\vec{k},m} V_{0m,\vec{k}}^{\vec{q},1m}(t)\left[V_{0m,\vec{k}}^{\vec{q},1m}(t')\right]^* G_{\vec{k}}^{(0)+-}(t,t')$$
$$\times G_{0m}^{(0)-+}(t',t)G_{1m}^{+-}(t,t'). \qquad (11)$$

The Green function $G_{1m}^{+-}(t,t')$ accounting for the finite lifetime of $N_2^*(^3\Sigma_u^+)$ is given by (time variables are suppressed and internal times are integrated over from $-\infty$ to $+\infty$):

$$G_{1m}^{+-} = \widetilde{G}_{1m}^{+-} + G_{1m}^{(0)R}\Sigma_{1m}^{++}G_{1m}^{+-}, \qquad (12)$$
$$\widetilde{G}_{1m}^{+-} = G_{1m}^{(0)+-} - G_{1m}^{(0)+-}\Sigma_{1m}^{--}G_{1m}^A, \qquad (13)$$
$$G_{1m}^A = G_{1m}^{(0)A} + G_{1m}^{(0)A}\Sigma_{1m}^A G_{1m}^A. \qquad (14)$$

Putting everything together, the final result is

$$\gamma_e = \frac{1}{2}\sum_m \int_{-\infty}^{\infty} dt_1 \int_{-\infty}^{\infty} dt_2 \left[\Delta_{1m}^A(t_1,t_2) + \Delta_{1m}^R(t_1,t_2)\right]$$
$$\times \left\{1 - \int_{-\infty}^{t_1} dt_1'' \int_{-\infty}^{t_1} dt_2'' \Delta_{1m}^A(t_1'',t_2'')\right.$$
$$\left.\times \widetilde{T}\exp\left[-\int_{t_2''}^{t_1} dt_1' \int_{t_2''}^{t_1} dt_2' \Delta_{1m}^A(t_1',t_2')\right]\right\}$$
$$\times T\exp\left[-\int_{-\infty}^{t_1} dt_1' \int_{-\infty}^{t_2} dt_2' \Delta_{1m}^R(t_1',t_2')\right] \qquad (15)$$

with $\Delta_{1m}^{A/R}(t_1,t_2)$ the advanced and retarded parts of

$$\Delta_{1m}(t_1,t_2) = \sum_{\vec{k},\vec{q}}\left[V_{0m,\vec{k}}^{\vec{q},1m}(t_1)\right]^* V_{0m,\vec{k}}^{\vec{q},1m}(t_2) n_{\vec{k}}$$
$$\times \exp[-i(\epsilon_{\vec{q}} + \epsilon_0 - \epsilon_1 - \epsilon_{\vec{k}})(t_1 - t_2)]. \qquad (16)$$

and T and $\widetilde{T}$ the chronological and antichronological time ordering operators.

Equation (15) is rather complex. However, we can show that $\Delta_{1m}(t_1,t_2)$ divergences at $t_1 = t_2$ for distances form the surface larger than $2r_{N_2}$. Hence, as far as the time integrations in (15) are concerned, $\Delta_{1m}(t_1,t_2)$ is basically local in time. The time ordering operators T and $\widetilde{T}$ can thus be neglected and γ_e numerically calculated [4].

4 References

[1] F. X. Bronold *et al.*, Phys. Rev. Lett. **101**, 175002 (2008).
[2] F. X. Bronold *et al.*, Eur. Phys. J. D **54**, 519 (2009).
[3] R. L. Heinisch *et al.*, arXiv:1001.4956 (2010).
[4] J. Marbach *et al.*, in preparation (2010).